Parameter-Inverted Image Pyramid Networks

Xizhou Zhu[2,1*], **Xue Yang**[1*], **Zhaokai Wang**[3,1*], **Hao Li**[4,1]
Wenhan Dou[2,5], **Junqi Ge**[2,5], **Lewei Lu**[5], **Yu Qiao**[1], **Jifeng Dai**[2,1†]

[1]OpenGVLab, Shanghai AI Laboratory [2]Tsinghua University
[3]Shanghai Jiao Tong University [4]The Chinese University of Hong Kong
[5]SenseTime Research

https://github.com/OpenGVLab/PIIP

Abstract

Image pyramids are commonly used in modern computer vision tasks to obtain multi-scale features for precise understanding of images. However, image pyramids process multiple resolutions of images using the same large-scale model, which requires significant computational cost. To overcome this issue, we propose a novel network architecture known as the Parameter-Inverted Image Pyramid Networks (PIIP). Our core idea is to use models with different parameter sizes to process different resolution levels of the image pyramid, thereby balancing computational efficiency and performance. Specifically, the input to PIIP is a set of multi-scale images, where higher resolution images are processed by smaller networks. We further propose a feature interaction mechanism to allow features of different resolutions to complement each other and effectively integrate information from different spatial scales. Extensive experiments demonstrate that the PIIP achieves superior performance in tasks such as object detection, segmentation, and image classification, compared to traditional image pyramid methods and single-branch networks, while reducing computational cost. Notably, when applying our method on a large-scale vision foundation model InternViT-6B, we improve its performance by 1%-2% on detection and segmentation with only 40%-60% of the original computation. These results validate the effectiveness of the PIIP approach and provide a new technical direction for future vision computing tasks.

1 Introduction

In modern computer vision, high-performance image perception systems increasingly rely on large-scale pre-trained models. These models typically consume tens of thousands to millions of GPU hours during pre-training [43, 44, 41]. To adapt these expensively pre-trained models for fine-grained image perception tasks (*e.g.*, detection [4, 63, 57, 56] and segmentation [19, 50]), researchers usually combine them with image pyramids [40, 37] or feature pyramids [27, 42, 34]. This combination is crucial for constructing multi-scale features essential for image understanding.

However, integrating these pre-trained models with image pyramids results in significant computational overhead. Image pyramids process the same image at multiple resolutions with the same large-scale model, causing the computational demands to increase quadratically with the image resolutions across all scales. Although feature pyramids [27, 16, 42] aim to reduce this overhead, in MS COCO challenges [28], most top-performing models [48, 14, 64, 7] still rely on image pyramids due to their superior performance. Therefore, it is necessary to reduce the computing resources for building image pyramids while maintaining high performance.

*Equal contribution. †Corresponding author: Jifeng Dai <daijifeng@tsinghua.edu.cn>.

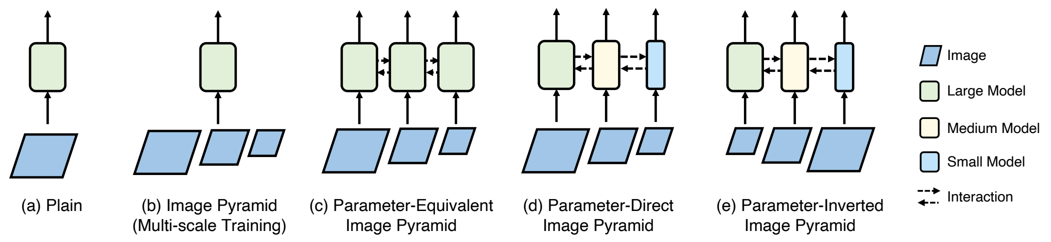
(a) Plain
(b) Image Pyramid (Multi-scale Training)
(c) Parameter-Equivalent Image Pyramid
(d) Parameter-Direct Image Pyramid
(e) Parameter-Inverted Image Pyramid
Image
Large Model
Medium Model
Small Model
Interaction

Figure 1: **Different parameter-resolution designs of image pyramid networks.** **(a)** Plain network which lacks multi-scale features. **(b)(c)** Inefficient image pyramid networks (shared weights / separate weights with interactions) using equivalently large networks for all scales. **(d)** Parameter-direct image pyramid network which processes high-resolution images with large models, leading to high computational cost. **(e)** Our efficient parameter-inverted image pyramid network (PIIP), which pairs models of increasing parameter sizes inversely with images of decreasing resolution. It delivers better performance than those of (b)(c)(d) with much lower computational cost.

To address this, our key idea is that it is unnecessary to employ vision models of equivalent size for feature extraction at all resolutions (Fig. 1(b-c)) or adopt a parameter-direct design (Fig. 1(d)). Features at different resolutions can complement each other through adequate feature fusion, thereby enhancing computational efficiency and avoiding redundant modeling of similar information. Specifically, for lower-resolution pyramid levels, the smaller images allow the efficient use of larger models to extract rich contextual and semantic features. The high-resolution branches need only provide the detail information missing from the lower-resolution features, instead of re-modeling existing semantic information. Thus, high-resolution features can focus on smaller receptive fields with less semantic information, making it possible to use smaller models to save computational resources.

Building on this strategy, a low-cost and high-performance image pyramid network can be constructed using a series of models with increasing parameter size, paired inversely with images of decreasing resolution, as shown in Fig. 1(e). Each resolution level should be able to directly leverage existing pre-trained vision foundation models for feature extraction, avoiding the large computational costs for training multi-scale image pyramid networks from scratch. In addition, sufficient feature interactions between different levels are also required to ensure the complementarity of features at different scales and avoid redundant feature extractions.

To this end, we propose Parameter-Inverted Image Pyramid Networks (PIIP) based on the complementarity of image features at different resolutions. Specifically, the network takes images at multiple scales as inputs, where higher resolution features are extracted through networks with fewer parameters for local detail perception, and lower resolution features are extracted with more parameters for global information extraction. Additionally, we introduce a feature interaction module that allows features between different resolutions to complement each other. This structure reduces the number of parameters of high-resolution branches and effectively integrates information from different receptive fields, significantly reducing computational costs without sacrificing performance.

We conduct experiments on object detection, instance segmentation, semantic segmentation and image classification. Our method achieves better performance while reducing computational costs, compared to traditional image pyramids and single-branch networks. These results validate the effectiveness of our multi-resolution feature interaction strategy and parameter-inverted paradigm and provide a new direction for future visual computing. Our contributions are as follows:

1) We propose a novel architecture named Parameter-Inverted Image Pyramid (PIIP) that enhances the multi-scale representational capability of vision backbones with high computation efficiency. The proposed architecture is capable of effectively and flexibly utilizing strong pre-trained vision foundation models without the need for extensive training from scratch.

2) We evaluate our method on classic vision tasks of object detection, instance segmentation, semantic segmentation, and image classification. Through combination of existing pre-trained models, our method surpasses single-branch models and other image pyramid methods with higher performance and lower computation cost.

3) To validate the generalizability of PIIP on large-scale vision foundation models, we apply PIIP to InternViT-6B [8], improving its performance on object detection and semantic segmentation by 1.9%

(55.7 AP^{b}) and 1.3% (59.7 mIoU) while reducing 43% and 58% of computational costs, respectively. We also provide extensive analysis and valuable insights on ablation and design guidelines for PIIP that may benefit future research.

2 Related Work

Image Pyramids and Feature Pyramids. Image pyramids and feature pyramids are two widely used techniques to enhance the multi-scale perceptive ability for downstream dense prediction tasks. Image pyramids [60, 39, 40, 37] resize the original image and extract features of different resolutions separately, allowing models to accurately detect objects of various scales. However, this technique significantly increases computational costs. Feature pyramids [27, 16, 42, 61, 34] represent another method for constructing multi-scale feature representations by merging low-resolution, semantically strong features with high-resolution, semantically weak features. Although significantly reducing computational costs, they cannot fully replace image pyramids when detecting very small or large objects [39]. Our proposed architecture integrates both image and feature pyramids and introduces the parameter-inverted paradigm to achieve efficient computation.

Multi-branch Architectures. Multi-branch architectures have been widely adopted to combine features from different resolutions in various computer vision tasks, including image classification [5], object detection [46, 25, 7, 52], semantic segmentation [58, 17] and multimodal dialogues [33, 21]. CrossViT [5] adopts a two-branch structure with different patch sizes to obtain inputs of various scales and different model sizes to balance the computational load. HRNet series [46, 58, 17] adopt a four-branch architecture, where the number of branches gradually increases as the layers deepen. However, they do not adopt the parameter inversion paradigm and cannot utilize existing pre-trained models. In contrast, we propose a general model architecture that supports the use of pre-trained models with different parameters to build efficient image pyramids.

Redundancy Reduction for Visual Models. Extensive studies focus on reducing computational redundancy for acceleration. Some work exploits the sparsity of images to accelerate model inference by reducing the number of visual tokens. Dynamic ViT [38] and AdaViT [35] design lightweight prediction modules to predict and prune less informative tokens. EViT [26] and Evo-ViT [55] compute attention scores for each token from class token to identify less informative tokens and adopt accelerated processing strategies for them. Other approaches focus on improving the model structure for efficient computation, such as attention mechanisms [47, 17, 3] or gradually reducing the spatial resolution as the number of layers increases [30, 49, 20]. Orthogonal to the above studies, we propose to use a parameter-inverted design to avoid using large models to process high-resolution images, greatly reducing the computation redundancy.

3 Parameter-Inverted Image Pyramid Networks

To construct efficient image pyramid networks, we employ a multi-branch structure to handle images of different resolutions with different sizes of models. As shown in Fig. 2, our architecture consists of three parts: multi-resolution branches, cross-branch interactions, and branch merging. Each branch uses an off-the-shelf pre-trained model to process images of different resolutions, where larger resolutions are processed by branches with fewer parameters. Cross-branch interactions are added every few blocks to fuse features across different feature scales. Branch merging combines the outputs from all branches to form a final output. We use the existing pre-trained ViTs [43, 44, 41] to initialize the branches, and initialize the interactions and branch merging from scratch.

3.1 Multi-Resolution Branches

The multi-resolution branches serve to extract representations from different image scales and semantic levels. The input image is first resized to different resolutions through bilinear interpolation, and then fed into corresponding branches to extract features at different scales. All the branches have the same number of blocks N, where each block contains one or multiple ViT [13] layers. Typically, blocks from different branches have different feature dimensions due to the pre-trained models, *e.g.* ViT-T, ViT-S and ViT-B. Branches with larger image sizes have a smaller number of parameters. For clarity, we refer to the branch with the largest number of parameters (with the smallest image size) as Branch 1, the second largest as Branch 2, and so on. The output of the i-th block of Branch j is

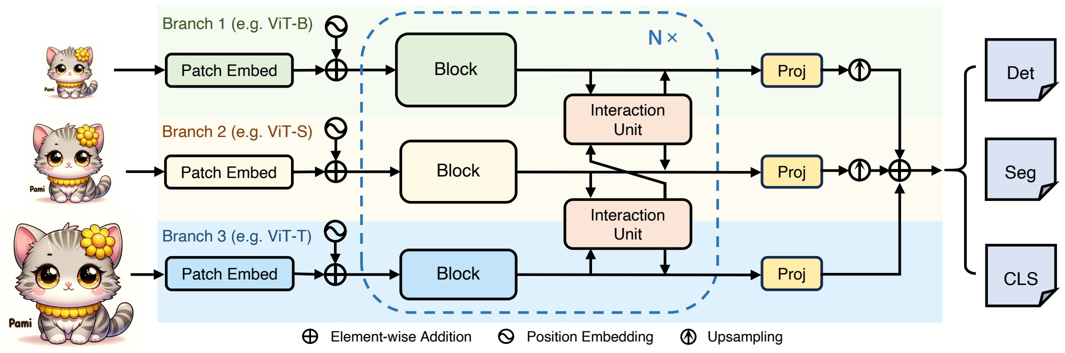

Figure 2: **Overall architecture of our method.** We use multi-resolution branches to process images of different resolutions, where larger images are handled by smaller models. Interaction Units build connections between branches. Branch merging combines the features of all branches to form the final output. Our architecture can leverage pre-trained models with different model sizes to build efficient image pyramids.

denoted as $\mathcal{F}_j^i \in \mathbb{R}^{H_j W_j / P_j^2 \times D_j}$, where H_j, W_j, P_j, D_j are the image height, image width, patch size, and feature dimension of Branch j, respectively.

3.2 Cross-branch Interactions

Branches of different resolutions focus on different spatial scales and semantic levels. To enhance the features of different scales, we propose the cross-branch interactions. Each cross-branch interaction consists of several interaction *units*, where each unit builds connections between outputs from two feature-scale adjacent branches. The structure of the interaction unit is shown in Fig. 3.

Specifically, for the outputs of the i-th block of Branch 1 and 2, denoted as $\mathcal{F}_1^i \in \mathbb{R}^{H_1 W_1 / P_1^2 \times D_1}$ and $\mathcal{F}_2^i \in \mathbb{R}^{H_2 W_2 / P_2^2 \times D_2}$, we perform two deformable cross-attention [63] between the two features, denoted as $\mathrm{Attention}(\cdot)$. Each cross attention is preceded by a linear layer $\mathrm{FC}(\cdot)$ to project the feature dimension of key and value into that of the query, *i.e.* from D_1 to D_2 or vice versa. A feed-forward network $\mathrm{FFN}(\cdot)$ is added after each cross attention to provide channel-wise feature fusion. The hidden dimension ratio of FFN is set to 0.25 to save computational overhead.

For the first cross-attention in the interaction unit, the interaction process can be formulated as:

$$\hat{\mathcal{F}}_1^i = \mathcal{F}_1^i + \gamma_1^i \mathrm{Attention}(\mathrm{norm}(\mathcal{F}_1^i), \mathrm{norm}(\mathrm{FC}(\mathcal{F}_2^i))), \tag{1}$$

$$\tilde{\mathcal{F}}_1^i = \hat{\mathcal{F}}_1^i + \tau_1^i \mathrm{FFN}(\mathrm{norm}(\hat{\mathcal{F}}_1^i)), \tag{2}$$

where $\mathrm{norm}(\cdot)$ is LayerNorm [1], τ_1^i and γ_1^i are learnable parameters, and $\tilde{\mathcal{F}}_1^i$ is the interaction output. τ_1^i and γ_1^i are initialized with $\mathbf{0}$ to ensure that the feature extraction of the original blocks (*i.e.* distribution of $\mathcal{F}_1^i$) will not be modified drastically due to the interactions, better utilizing the pre-trained weights.

Similarly, the second cross-attention is performed by switching the query and key/value to obtain $\tilde{\mathcal{F}}_2^i$. The outputs $\tilde{\mathcal{F}}_1^i$ and $\tilde{\mathcal{F}}_2^i$ are used for subsequent feature extractions. We only construct interaction units between each pair of feature-scale adjacent branches, such as Branch 1 & Branch 2 and Branch 2 & Branch 3.

3.3 Branch Merging

The final feature maps of all branches $\tilde{\mathcal{F}}_j^N$ have different spatial shapes and feature dimensions, where spatially larger feature maps have fewer feature dimensions. A single feature map fails to provide multi-scale semantic features, so we employ the branch merging module to merge the outputs of all branches into a single feature map.

As shown in Fig. 2, all branch outputs are first projected to the feature dimension of Branch 1 (the largest feature dimension) with $\mathrm{Proj}(\cdot)$. Then, all branch outputs are upsampled by bilinear interpolation $\mathrm{Upsample}(\cdot)$ into the feature map size of the last branch (the largest feature map size).

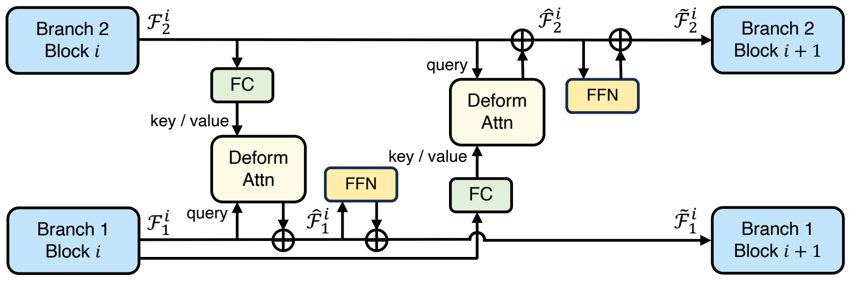

Figure 3: Structure of an interaction unit.

Finally, these outputs, with the same spatial shape and feature dimension, are added together with learnable scalar weights w_j to form the final output. This process can be formulated as:

$$\tilde{\mathcal{F}}_j^{\text{out}} = \text{Upsample}(\text{Proj}(\tilde{\mathcal{F}}_j^N)), \tag{3}$$

$$\mathcal{F}^{\text{out}} = \sum_{j=1}^{M} w_j \tilde{\mathcal{F}}_j^{\text{out}}, \tag{4}$$

where M is the number of branches. $\mathcal{F}^{\text{out}}$ is the final feature map, which has the largest feature resolution and also the largest feature dimension across all branches.

For object detection and semantic segmentation, $\text{Proj}(\cdot)$ is a two-convolution layer with GroupNorm [51], and the final output $\mathcal{F}^{\text{out}}$ is used for feature pyramid network [27] similar to ViTDet [23].

For image classification, we do not use the branch merging module, but instead append the original classification heads of the pre-trained models after each branch. The final classification score is the average of the output logits of all branches. We observe that using the pre-trained heads can speed up convergence compared to using a randomly initialized head after a branch merging module.

4 Experiments

4.1 Implementation Details

For comparison with Base-size models, we use pre-trained ViT-T/S/B as the branches to construct three-branch PIIP network, namely PIIP-TSB. Similarly, ViT-S/B/L are used to construct PIIP-SBL to match the computation of Large-size models. We also construct four-branch PIIP-TSBL with ViT-T/S/B/L. We set the number of interactions (each with 2 interaction units as shown in Fig. 2) N to 12, *i.e.* after every layer for ViT-T/S/B or after every two layers for ViT-L. We construct multiple variants of three-branch and four-branch models with different resolution configurations. For combinations with an inconsistent number of layers, we will use a larger learning rate decay for the backbone with fewer layers. For example, for ViT-S/B (12 layers) and ViT-L (24 layers), the learning rate decay for ViT-S/B is set to be twice that of ViT-L (24/12=2).

For object detection and segmentation, we use ViT-S/B/L pre-trained on ImageNet [11] from DeiT III [44], ViT-T from DeiT [43]. ViT-H from MAE [18] and InternViT-6B [8] are used for 6B-scale experiments. For all PIIP-SBL models, we use the ImageNet-21K 384-resolution pre-trained weights to compare with previous approaches. We adopt AdamW [32] optimizer with layer-wise learning rate decay [2] to train the model on 8 NVIDIA A800 GPUs. For image classification, in Base-size experiments we use pre-trained ViT-T/S/B weights from DeiT [43]. In Large-size experiments, since DeiT does not provide ViT-L models, we use ImageNet-21K pre-trained ViT-S/B/L weights from [41].

We use the FLOPs calculation script from MMDetection [6], with our modifications to accurately calculate FLOPs of modules like self-attention and deformable attention. The script is released along with the training code. We have also manually verified the calculations using formulas, and the results are consistent with those produced by the script.

Table 1: **Comparison with baseline on COCO val2017.** We report the number of parameters and FLOPs of the backbone. Underline indicates FLOPs or metrics on par with the baseline. AP^b and AP^m represent box AP and mask AP, respectively.

Model	**Resolution**	**#Param**	**#FLOPs**	**Mask R-CNN 1× schedule**					
				AP^b	AP^b_{50}	AP^b_{75}	AP^m	AP^m_{50}	AP^m_{75}
ViTDet-B [23]	1024	90M	463G	43.8	67.6	47.7	39.9	63.6	42.2
PIIP-TSB (ours)	1120/896/448	146M	243G	43.9	65.7	47.5	38.6	61.8	40.6
	1568/896/448	147M	287G	45.0	67.0	48.7	40.2	63.8	42.6
	1568/1120/672	149M	453G	**46.6**	68.4	51.1	**41.4**	65.2	44.3
ViTDet-L [23]	1024	308M	1542G	46.8	70.8	51.4	42.5	67.3	45.3
PIIP-SBL (ours)	1120/672/448	493M	727G	46.7	69.0	50.6	40.8	65.2	42.8
	1344/896/448	495M	1002G	48.2	71.0	52.8	42.5	67.3	45.4
	1568/896/672	497M	1464G	49.4	71.9	53.9	43.7	68.4	46.6
PIIP-TSBL (ours)	1344/896/672/448	506M	755G	46.9	69.9	50.6	41.6	65.9	44.1
	1568/1120/672/448	507M	861G	48.2	70.5	52.7	42.8	66.9	45.6
	1792/1568/1120/448	512M	1535G	**49.6**	72.4	54.2	**44.2**	69.2	47.5

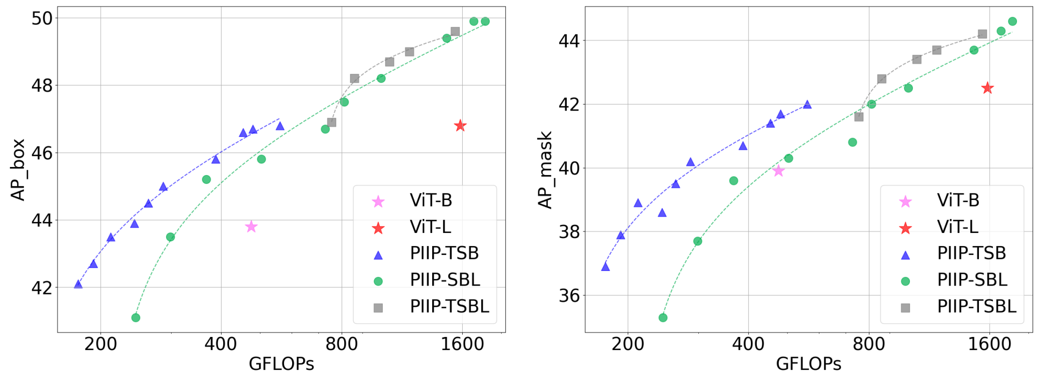

(a) Object detection (b) Instance segmentation

Figure 4: **Performance of different PIIP variants by adjusting input resolutions.** Detailed resolution configuration and results are provided in the appendix.

4.2 Object Detection and Instance Segmentation

Settings. The MS COCO [28] dataset is used to evaluate the performance on object detection and instance segmentation. We use three detectors, including Mask R-CNN [19], Cascade R-CNN [4] and DINO [59], based on MMDetection [6]. Following common practices [7], we adopt 1× (12 epochs) or 3× (36 epochs) training schedules and use window attention [23] to save time and memory. The total batch size is 16, and the initial learning rate and weight decay are 1e-4 and 0.05.

Effectiveness of Parameter-Inverted Image Pyramid. To demonstrate the performance and computational advantages of the Parameter-Inverted Image Pyramid (PIIP) Networks, we perform validation on two baseline models ViTDet-B and ViTDet-L [23] in Tab. 1. Taking the three-branch structure as an example, while maintaining similar performance with ViTDet-B, our PIIP-TSB reduces the computational cost by 47.5% (243G vs. 463G) and 38.0% (287G vs. 463G) in object detection and instance segmentation tasks respectively. Similarly, compared with ViTDet-L, our PIIP-SBL reduces the computational cost by about 52.9% (727G vs. 1,542G) and 35.0% (1,002G vs. 1,542G) in the above two tasks respectively. On the other hand, with similar computational cost as the baseline, PIIP-TSB and PIIP-SBL improve the object detection performance by 2.8% and 2.6%, respectively, and instance segmentation by 1.5% and 1.2%, compared to ViTDet-B and ViTDet-L. To better illustrate the above conclusion, we depict the trend between the computational cost and performance of different PIIP model combinations by adjusting the input resolution, as shown in Fig. 4. Furthermore, when we use the four-branch structures, the curve in the figure is slightly better than that of the three-branch structure.

Table 2: **Object detection and instance segmentation performance on COCO val2017.** 'MS' means using AutoAugment [10] for multi-scale training. Large-size models use ViT weights trained on ImageNet-21K. The ViTDet-B and ViTDet-L results (and other entries) are cited from ViT-Adapter [7]. PIIP-SBL with Mask R-CNN uses higher resolutions than those in Tab. 1, as reported in Tab. 12. For PIIP-TSB with Mask R-CNN, higher resolutions (1568/896/672 -> 1792/1344/672) and a larger window size (14 -> 28) are used, compared with the results in the Tab. 1.

Method	AP^b	AP^b_{50}	AP^b_{75}	AP^m	AP^m_{50}	AP^m_{75}
	Mask R-CNN 1× schedule					
PVTv2-B5 [49]	47.4	68.6	51.9	42.5	65.7	46.0
ViT-B [24]	42.9	65.7	46.8	39.4	62.6	42.0
ViTDet-B [23]	43.2	65.8	46.9	39.2	62.7	41.4
Swin-B [30]	46.9	-	-	42.3	-	-
ViT-Adapter-B [7]	47.0	68.2	51.4	41.8	65.1	44.9
PIIP-TSB (ours)	47.9	70.2	52.5	42.6	67.2	45.5
ViT-L [24]	45.7	68.9	49.4	41.5	65.6	44.6
ViTDet-L [23]	46.2	69.2	50.3	41.4	65.8	44.1
ViT-Adapter-L [7]	48.7	70.1	53.2	43.3	67.0	46.9
PIIP-SBL (ours)	49.9	72.8	54.7	44.6	69.3	47.9
	DINO + MS 3× schedule					
PIIP-SBL-3× (ours)	57.9	76.9	63.3	-	-	-

Method	AP^b	AP^b_{50}	AP^b_{75}	AP^m	AP^m_{50}	AP^m_{75}
	Cascade R-CNN 1× schedule					
Swin-L [30]	51.8	71.0	56.2	44.9	68.4	48.9
ConvNeXt-L [31]	53.5	72.8	58.3	46.4	70.2	50.2
PIIP-SBL (ours)	53.6	73.3	57.9	46.3	70.3	50.0
	Cascade R-CNN 3× + MS schedule					
Swin-B [30]	51.9	70.9	57.0	-	-	-
Shuffle-B [22]	52.2	71.3	57.0	-	-	-
ViT-B [24]	50.1	69.3	54.3	-	-	-
ViT-Adapter-B [7]	52.1	70.6	56.5	-	-	-
PIIP-TSB (ours)	53.1	72.3	57.4	46.5	70.1	51.1
Swin-L [30]	53.9	72.4	58.8	46.7	70.1	50.8
RepLKNet-31L [12]	53.9	72.5	58.6	46.5	70.0	50.6
ConvNeXt-L [31]	54.8	73.8	59.8	47.6	71.3	51.7
PIIP-SBL (ours)	54.5	73.8	59.1	47.7	71.6	52.1

Table 3: **Experiments on the large-scale vision foundation model InternViT-6B.**

Model	**#Param**	**Mask R-CNN 1× schedule**				**UperNet 160k**		
		#FLOPs	Resolution	AP^b	AP^m	Crop Size	#FLOPs	mIoU
InternViT-6B [8]	5919M	24418G	1024	53.8	48.1	$\underline{512}^2$	6105G	58.36
PIIP-LH6B (ours)	7269M	5643G	1280/1024/256	53.5	47.5	640/$\underline{512}^2$/192	1903G	57.82
	7271M	10368G	1280/1024/512	54.4	47.8	640/$\underline{512}^2$/256	2592G	58.42
	7273M	13911G	1280/1024/640	**55.7**	**49.0**	640/$\underline{512}^2$/384	4560G	**59.65**

Results with Base-size and Large-size models. As shown in Tab. 2, combined with Mask R-CNN, PIIP achieves higher performance than ViT-Adapter by a considerable margin, about 0.9% and 1.2% on AP^b. With a more powerful detector Cascade R-CNN and stronger training schedule (3× + MS), PIIP-TSB and PIIP-SBL achieve competitive performance of 53.1% and 54.5% AP^b, respectively. Finally, we achieve 57.9% AP^b with the DINO [59] detector. These results demonstrate the scalability of PIIP.

Results with InternViT-6B. We further examine PIIP on an extremely large vision foundation model InternViT-6B [8]. As can be seen from Tab. 3, PIIP-LH6B finally achieves 55.7% AP^b when using Mask R-CNN 1× training schedule. In addition, our PIIP can save nearly 43% of the computation and achieve better performance than the single-branch InternViT-6B by 1.9% on AP^b and 0.9% on AP^m.

4.3 Semantic Segmentation

Settings. We use UperNet [54] as the basic framework to train on the ADE20K [62] dataset based on MMSegmentation [9]. We follow the settings of [30] to train the model for 160k iterations. The batch size, initial learning rate and weight decay are 16, 4e-5 and 0.05.

Results with Base-size and Large-size models. In Tab. 5, PIIP can achieve better performance with fewer computations compared with single-branch baselines. In Tab. 4, we compare PIIP with state-of-the-art segmentation backbones. PIIP-TSB attains 51.6% mIoU with UperNet, exceeding InternImage-B [48] by 1.4%. Similarly, PIIP-SBL yields 54.3% mIoU, which is outstanding compared to counterparts like ConvNeXt-XL [31] and InternImage-L [48].

Results with InternViT-6B. As shown in Tab. 3, similar to the conclusions obtained in the object detection experiment, our method achieves better performance than the InternViT-6B baseline with less computation. PIIP-LH6B finally achieves 59.65% mIoU without using additional optimization techniques.

Table 4: **Semantic segmentation performance on ADE20K using UperNet.**

Method	Crop Size	mIoU
Swin-B [30]	$\underline{512^2}$	48.1
ConvNeXt-B [31]	$\underline{512^2}$	49.1
RepLKNet-31B [12]	$\underline{512^2}$	49.9
SLaK-B [29]	$\underline{512^2}$	50.2
InternImage-B [48]	$\underline{512^2}$	50.2
PIIP-TSB (ours)	896/$\underline{448^2}$/336	**51.6**
Swin-L [30]	$\underline{640^2}$	52.1
RepLKNet-31L [12]	$\underline{640^2}$	52.4
ConvNeXt-L [31]	$\underline{640^2}$	53.2
ConvNeXt-XL [31]	$\underline{640^2}$	53.6
InternImage-L [48]	$\underline{640^2}$	53.9
PIIP-SBL (ours)	1120/$\underline{448^2}$/336	**54.3**

Table 5: **Comparison with baseline on ADE20K using UperNet.**

Method	Crop Size	#FLOPS	mIoU
ViT-B	$\underline{640^2}$	159G	51.0
PIIP-TSB (ours)	896/$\underline{448^2}$/336	118G	51.6
ViT-L	$\underline{640^2}$	545G	53.6
PIIP-SBL (ours)	1120/$\underline{448^2}$/336	456G	54.3

Table 6: **Image classification performance on ImageNet.** Underline indicates FLOPs or metrics on par with the baseline.

Model	Resolution	#FLOPs	Top-1 Acc
DeiT-B [43]	224	17.2G	81.8
PIIP-TSB (ours)	368/192/128	$\underline{\text{17.4G}}$	82.1
ViT-L [41]	224	61.6G	84.0
ViT-L [41] (our impl.)	224	61.6G	85.2
PIIP-SBL (ours)	320/160/96	39.0G	$\underline{85.2}$
PIIP-SBL (ours)	384/192/128	$\underline{\text{61.2G}}$	85.9

Table 7: **Ablation on image pyramid and parameter-inverted design.** 'PI', 'IP' and 'Inter.' represent parameter-inverted, image pyramid and interactions. 'MS' means multi-scale training, following [10].

Figure	Branches	PI	IP	Inter.	Resolution	#Param	#FLOPs	Mask R-CNN 1× schedule					
								AP^b	AP^b_{50}	AP^b_{75}	AP^m	AP^m_{50}	AP^m_{75}
Fig. 1(a)	B				1024	90M	463G	43.8	67.6	47.7	39.9	63.6	42.2
Fig. 1(b)	B		✓		MS	90M	463G	44.8	69.2	49.1	41.0	65.8	43.9
-	BBB		✓		896/448/224	262M	369G	43.3	65.8	46.6	37.9	61.5	39.6
-	BBB		✓		896/672/224	263M	457G	43.8	66.3	47.3	38.2	62.2	39.7
Fig. 1(c)	BBB		✓	✓	896/448/224	341M	466G	44.5	66.5	48.2	38.7	62.6	40.6
-	TSB			✓	896/896/896	148M	468G	44.6	66.4	48.3	39.0	62.7	41.4
Fig. 1(d)	TSB		✓	✓	448/672/896	147M	452G	42.6	64.2	45.6	36.5	59.5	38.0
Fig. 1(e)	TSB	✓	✓	✓	1568/1120/672	149M	453G	**46.6**	68.4	51.1	**41.4**	65.2	44.3
Fig. 1(a)	L				1024	308M	1542G	46.8	70.8	51.4	42.5	67.3	45.3
Fig. 1(c)	LLL		✓	✓	896/448/224	1053M	1458G	46.9	69.7	51.2	40.8	65.3	43.3
-	SBL			✓	848/848/848	495M	1539G	47.2	69.4	51.0	41.1	65.4	43.7
Fig. 1(e)	SBL	✓	✓	✓	1568/896/672	497M	1464G	**49.4**	71.9	53.9	**43.7**	68.4	46.6

4.4 Image Classification

Settings. We load the pre-trained models for each branch and train the model for 20 epochs on ImageNet-1K [11]. The batch size, initial learning rate and weight decay are 1024, 3e-5 and 0.1. The learning rate for the random initialized interactions is 10 times the base learning rate, *i.e.* 3e-4. The other settings mainly follow the fine-tuning recipe of [44] and are provided in the appendix.

Results. As shown in Tab. 6, when compared with the DeiT baseline, our PIIP-SBL reduces the computational cost by 36.7% (39.0G vs. 61.6G) while maintaining the performance. When using a similar computational cost as the baseline models, PIIP-TSB and PIIP-SBL improve the top-1 accuracy by 0.3% and 0.7%, respectively.

4.5 Ablation Study

Superiority of parameter-inverted image networks. We evaluate the effectiveness of the image pyramid and parameter-inverted design by comparing our method with other methods, *e.g.* designs in Fig. 1. First of all, a single-branch with multi-scale training is the simplest image pyramid practice, as shown in Tab. 7. Compared with the baseline model, its performance improvement is limited (44.8% vs. 43.8%). Secondly, we conduct experiments by controlling the scale of the branch model and the input resolution while ensuring that the total computational cost is close. Specifically, when using the same input image resolution, the combination of models of different sizes does not bring

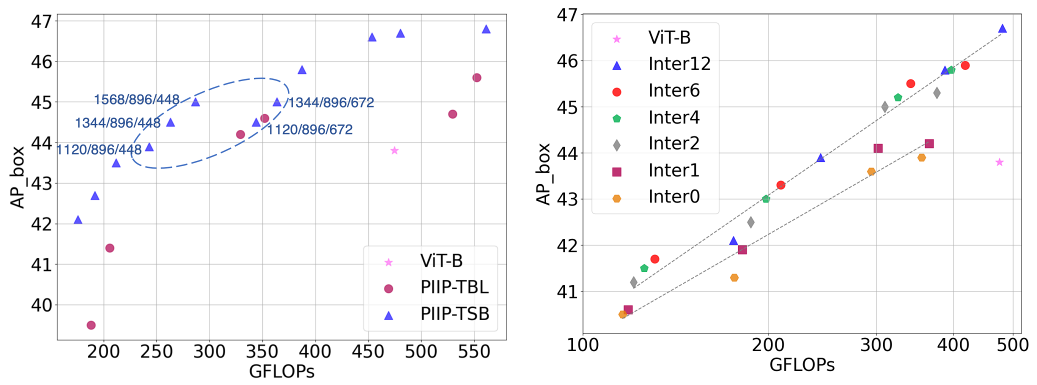

(a) Variants with different resolutions (b) Number of interactions

Figure 5: **Ablation on model variants and number of interactions.**

Table 8: **Ablation on Branch Merging on COCO val2017.** We use PIIP-TSB 1568/896/672.

Out Branch	AP^b	AP^m
B	43.1	37.0
S	44.7	39.1
T	45.6	40.6
B+S	45.4	39.8
B+T	46.3	41.1
S+T	46.2	40.9
B+S+T	**46.6**	**41.4**

Table 9: **Ablation on attention type and number of interactions** with PIIP-TSB 1120/896/448.

#Inter.	Regular Attention					Deformable Attention				
	#FLOPs	AP^b	AP^b_l	AP^b_m	AP^b_s	#FLOPs	AP^b	AP^b_l	AP^b_m	AP^b_s
0	176G	41.3	59.0	44.6	22.5	176G	41.3	59.0	44.6	22.5
1	211G	41.1	59.1	44.9	22.6	182G	41.9	59.8	45.5	22.4
2	245G	41.7	59.5	45.2	22.7	187G	42.5	60.5	46.4	23.1
4	315G	41.6	59.2	45.3	22.8	198G	43.0	61.0	47.3	23.3
6	384G	42.1	59.7	45.8	23.2	210G	43.3	61.8	46.9	23.6
12	592G	42.0	60.0	45.9	23.1	243G	**43.9**	62.4	47.9	24.4

significant improvements to detection performance. Correspondingly, when the three branches use the same model (*e.g.* BBB), the input image resolution is adjusted to the pyramid structure. The performance of the final model is slightly improved on AP^b (44.5% vs. 43.8%), but the AP^m drops significantly (38.7% vs 39.9%) due to the reduction of the maximum resolution. The former demonstrates the importance of the image pyramid, and the latter further demonstrates the need for the image pyramid to maintain a larger image scale range, which is especially essential for instance segmentation. Drawing on experience, parameter-inverted image networks are an efficient design method that can meet the above requirements, especially when compared to its opposite configuration parameter-direct image pyramid, *i.e.* TSB with 448/672/896 resolution (46.6% vs. 42.6%). As shown in Tab. 7, with less computation than the baseline, the model can support image inputs in the maximum range from 672 to 1,568, and the performance is significantly improved.

Design guidelines for parameter-inverted image networks. Through extensive practice, there are two empirical design guidelines when scaling up the model: 1) Prioritize increasing the image resolution of the largest image branch: as shown in the blue dashed circle in Fig. 5(a), the input resolution of the largest image branch is greatly increased without causing a sharp increase in the total computational cost. 2) The largest model does not need to exceed the compared baseline model: the introduction of larger models will limit the resolution range of the image pyramid, *e.g.* TSB is more cost-effective than TBL according to Fig. 5(a).

Branch merging. Experiments in Tab. 8 prove that branch merging of all branches yields the best performance by providing multi-scale semantically rich features, compared to only using feature maps from single or partial branches.

Attention type. The core of information interaction between branches is cross-attention. We adopt PIIP-TSB with resolution 1120/896/448 as the basic model and investigate two different attention mechanisms. As shown in Tab. 9, deformable attention [53] with linear complexity can significantly improve the performance of the model without substantially increasing the computational cost. We end up using deformable attention as the default configuration. Notably, it can be replaced by other more advanced attention mechanisms in the future to further boost performance.

Table 10: **Ablation on interaction directions** with PIIP-TSB under resolution 1120/896/448.

Type	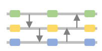	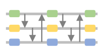	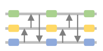	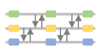	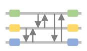
#FLOPs	210G	230G	230G	243G	283G
AP^b	43.5	43.2	43.6	43.9	44.0
AP^m	38.7	38.3	38.6	38.6	38.7

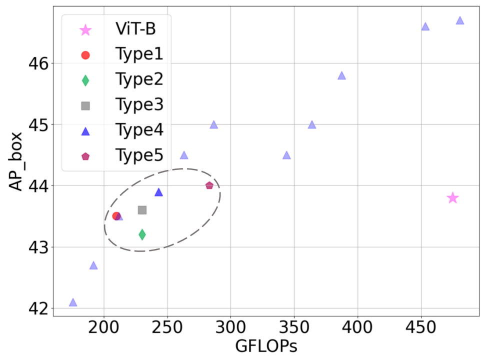

Figure 6: **Performance of different interaction directions.**

Number of interactions. As shown in Tab. 9, no matter which attention mechanism is used, the increase in the number of interactions will improve the performance of the model to varying degrees. Since it also increases the computational cost, we further explore the cost-effectiveness of different numbers of interactions. We conduct experiments with different resolution combinations on models with different numbers of interactions, and the scatter plot of all results is shown in Fig. 5(b). It can be seen that when the number of interactions is small (less than 2), the growth trend of model performance with the increase in computational cost is relatively slow. We attribute this to too few interactions and insufficient information complementation between branches. Therefore, we use 12 interactions by default. Note that as the model size increases (*e.g.* more layers), the number of interactions can also increase accordingly.

Interaction direction between branches. We compare five different interaction directions in Tab. 10. Considering both the computational cost and performance, we finally choose the fourth method, *i.e.* bidirectional connections of adjacent branches, as the default choice. As can be seen from Fig. 6, all the interaction directions achieve a satisfactory performance-computation balance, validating their ability to improve communication between branches.

5 Conclusion

This paper introduces the Parameter-Inverted Image Pyramid Networks (PIIP) to address the computational challenges of traditional image pyramids. With the parameter-inverted design and feature interaction mechanism, PIIP effectively balances computational efficiency and performance. Extensive experiments on detection, segmentation and classification tasks demonstrate that PIIP outperforms traditional methods and single-branch networks while reducing computational costs, providing an efficient and effective framework of multi-scale feature integration for future research.

Limitations. While our method manages to save computation, its memory consumption is higher than single-branch models due to the increase of parameter count. Our current method only focuses on ViT-based models. PIIP with hierarchical networks (*e.g.* CNN) or heterogeneous structures (*e.g.* CNN for some branches and ViT for other branches) remain unexplored for future work.

Acknowledgement

This work is supported by the National Key R&D Program of China (NO. 2022ZD0161300, NO. 2022ZD0160100), by the National Natural Science Foundation of China (62376134).

References

[1] Jimmy Lei Ba, Jamie Ryan Kiros, and Geoffrey E Hinton. Layer normalization. *arXiv preprint arXiv:1607.06450*, 2016.

[2] Hangbo Bao, Li Dong, Songhao Piao, and Furu Wei. Beit: Bert pre-training of image transformers. In *International Conference on Learning Representations*, 2021.

[3] Han Cai, Junyan Li, Muyan Hu, Chuang Gan, and Song Han. Efficientvit: Lightweight multi-scale attention for high-resolution dense prediction. In *Proceedings of the IEEE/CVF International Conference on Computer Vision*, pages 17302–17313, 2023.

[4] Zhaowei Cai and Nuno Vasconcelos. Cascade r-cnn: Delving into high quality object detection. In *Proceedings of the IEEE conference on computer vision and pattern recognition*, pages 6154–6162, 2018.

[5] Chun-Fu Richard Chen, Quanfu Fan, and Rameswar Panda. Crossvit: Cross-attention multi-scale vision transformer for image classification. In *Proceedings of the IEEE/CVF international conference on computer vision*, pages 357–366, 2021.

[6] Kai Chen, Jiaqi Wang, Jiangmiao Pang, Yuhang Cao, Yu Xiong, Xiaoxiao Li, Shuyang Sun, Wansen Feng, Ziwei Liu, Jiarui Xu, Zheng Zhang, Dazhi Cheng, Chenchen Zhu, Tianheng Cheng, Qijie Zhao, Buyu Li, Xin Lu, Rui Zhu, Yue Wu, Jifeng Dai, Jingdong Wang, Jianping Shi, Wanli Ouyang, Chen Change Loy, and Dahua Lin. MMDetection: Open mmlab detection toolbox and benchmark. *arXiv preprint arXiv:1906.07155*, 2019.

[7] Zhe Chen, Yuchen Duan, Wenhai Wang, Junjun He, Tong Lu, Jifeng Dai, and Yu Qiao. Vision transformer adapter for dense predictions. In *International Conference on Learning Representations*, 2022.

[8] Zhe Chen, Jiannan Wu, Wenhai Wang, Weijie Su, Guo Chen, Sen Xing, Muyan Zhong, Qinglong Zhang, Xizhou Zhu, Lewei Lu, Bin Li, Ping Luo, Tong Lu, Yu Qiao, and Jifeng Dai. Internvl: Scaling up vision foundation models and aligning for generic visual-linguistic tasks. In *Proceedings of the IEEE/CVF conference on computer vision and pattern recognition*, 2024.

[9] MMSegmentation Contributors. MMSegmentation: Openmmlab semantic segmentation toolbox and benchmark. `https://github.com/open-mmlab/mmsegmentation`, 2020.

[10] Ekin D Cubuk, Barret Zoph, Dandelion Mane, Vijay Vasudevan, and Quoc V Le. Autoaugment: Learning augmentation policies from data. *arXiv preprint arXiv:1805.09501*, 2018.

[11] Jia Deng, Wei Dong, Richard Socher, Li-Jia Li, Kai Li, and Li Fei-Fei. Imagenet: A large-scale hierarchical image database. In *Proceedings of the IEEE/CVF conference on computer vision and pattern recognition*, pages 248–255, 2009.

[12] Xiaohan Ding, Xiangyu Zhang, Jungong Han, and Guiguang Ding. Scaling up your kernels to 31x31: Revisiting large kernel design in cnns. In *Proceedings of the IEEE/CVF conference on computer vision and pattern recognition*, pages 11963–11975, 2022.

[13] Alexey Dosovitskiy, Lucas Beyer, Alexander Kolesnikov, Dirk Weissenborn, Xiaohua Zhai, Thomas Unterthiner, Mostafa Dehghani, Matthias Minderer, Georg Heigold, Sylvain Gelly, Jakob Uszkoreit, and Neil Houlsby. An image is worth 16x16 words: Transformers for image recognition at scale. *International Conference on Learning Representations*, 2021.

[14] Yuxin Fang, Wen Wang, Binhui Xie, Quan Sun, Ledell Wu, Xinggang Wang, Tiejun Huang, Xinlong Wang, and Yue Cao. Eva: Exploring the limits of masked visual representation learning at scale. In *Proceedings of the IEEE/CVF Conference on Computer Vision and Pattern Recognition*, pages 19358–19369, 2023.

[15] Inc. Flickr. Flickr terms & conditions of use. `https://www.flickr.com/help/terms`.

[16] Golnaz Ghiasi, Tsung-Yi Lin, and Quoc V Le. Nas-fpn: Learning scalable feature pyramid architecture for object detection. In *Proceedings of the IEEE/CVF conference on computer vision and pattern recognition*, pages 7036–7045, 2019.

[17] Jiaqi Gu, Hyoukjun Kwon, Dilin Wang, Wei Ye, Meng Li, Yu-Hsin Chen, Liangzhen Lai, Vikas Chandra, and David Z Pan. Hrvit: Multi-scale high-resolution vision transformer. *arXiv preprint arXiv:2111.01236*, 2021.

[18] Kaiming He, Xinlei Chen, Saining Xie, Yanghao Li, Piotr Dollár, and Ross Girshick. Masked autoencoders are scalable vision learners. In *Proceedings of the IEEE/CVF conference on computer vision and pattern recognition*, pages 16000–16009, 2022.

[19] Kaiming He, Georgia Gkioxari, Piotr Dollár, and Ross Girshick. Mask r-cnn. In *Proceedings of the IEEE/CVF International Conference on Computer Vision*, pages 2961–2969, 2017.

[20] Byeongho Heo, Sangdoo Yun, Dongyoon Han, Sanghyuk Chun, Junsuk Choe, and Seong Joon Oh. Rethinking spatial dimensions of vision transformers. In *Proceedings of the IEEE/CVF international conference on computer vision*, pages 11936–11945, 2021.

[21] Wenyi Hong, Weihan Wang, Qingsong Lv, Jiazheng Xu, Wenmeng Yu, Junhui Ji, Yan Wang, Zihan Wang, Yuxiao Dong, Ming Ding, et al. Cogagent: A visual language model for gui agents. *arXiv preprint arXiv:2312.08914*, 2023.

[22] Zilong Huang, Youcheng Ben, Guozhong Luo, Pei Cheng, Gang Yu, and Bin Fu. Shuffle transformer: Rethinking spatial shuffle for vision transformer. *arXiv preprint arXiv:2106.03650*, 2021.

[23] Yanghao Li, Hanzi Mao, Ross Girshick, and Kaiming He. Exploring plain vision transformer backbones for object detection. In *European Conference on Computer Vision*, pages 280–296. Springer, 2022.

[24] Yanghao Li, Saining Xie, Xinlei Chen, Piotr Dollar, Kaiming He, and Ross Girshick. Benchmarking detection transfer learning with vision transformers. *arXiv preprint arXiv:2111.11429*, 2021.

[25] Tingting Liang, Xiaojie Chu, Yudong Liu, Yongtao Wang, Zhi Tang, Wei Chu, Jingdong Chen, and Haibin Ling. Cbnet: A composite backbone network architecture for object detection. *IEEE Transactions on Image Processing*, 31:6893–6906, 2022.

[26] Youwei Liang, Chongjian Ge, Zhan Tong, Yibing Song, Jue Wang, and Pengtao Xie. Not all patches are what you need: Expediting vision transformers via token reorganizations. In *International Conference on Learning Representations*, 2022.

[27] Tsung-Yi Lin, Piotr Dollár, Ross Girshick, Kaiming He, Bharath Hariharan, and Serge Belongie. Feature pyramid networks for object detection. In *Proceedings of the IEEE/CVF conference on computer vision and pattern recognition*, pages 2117–2125, 2017.

[28] Tsung-Yi Lin, Michael Maire, Serge Belongie, James Hays, Pietro Perona, Deva Ramanan, Piotr Dollár, and C Lawrence Zitnick. Microsoft coco: Common objects in context. In *Proceedings of the European conference on computer vision*, pages 740–755, 2014.

[29] Shiwei Liu, Tianlong Chen, Xiaohan Chen, Xuxi Chen, Qiao Xiao, Boqian Wu, Tommi Kärkkäinen, Mykola Pechenizkiy, Decebal Mocanu, and Zhangyang Wang. More convnets in the 2020s: Scaling up kernels beyond 51x51 using sparsity. *arXiv preprint arXiv:2207.03620*, 2022.

[30] Ze Liu, Yutong Lin, Yue Cao, Han Hu, Yixuan Wei, Zheng Zhang, Stephen Lin, and Baining Guo. Swin transformer: Hierarchical vision transformer using shifted windows. In *Proceedings of the IEEE/CVF International Conference on Computer Vision*, pages 10012–10022, 2021.

[31] Zhuang Liu, Hanzi Mao, Chao-Yuan Wu, Christoph Feichtenhofer, Trevor Darrell, and Saining Xie. A convnet for the 2020s. In *Proceedings of the IEEE/CVF conference on computer vision and pattern recognition*, pages 11976–11986, 2022.

[32] Ilya Loshchilov and Frank Hutter. Decoupled weight decay regularization. In *International Conference on Learning Representations*, 2017.

[33] Gen Luo, Yiyi Zhou, Yuxin Zhang, Xiawu Zheng, Xiaoshuai Sun, and Rongrong Ji. Feast your eyes: Mixture-of-resolution adaptation for multimodal large language models. *arXiv preprint arXiv:2403.03003*, 2024.

[34] Yihao Luo, Xiang Cao, Juntao Zhang, Jingjuan Guo, Haibo Shen, Tianjiang Wang, and Qi Feng. Ce-fpn: enhancing channel information for object detection. *Multimedia Tools and Applications*, 81(21):30685–30704, 2022.

[35] Lingchen Meng, Hengduo Li, Bor-Chun Chen, Shiyi Lan, Zuxuan Wu, Yu-Gang Jiang, and Ser-Nam Lim. Adavit: Adaptive vision transformers for efficient image recognition. In *Proceedings of the IEEE/CVF Conference on Computer Vision and Pattern Recognition*, pages 12309–12318, 2022.

[36] MIT. Ade20k terms & conditions of use. https://groups.csail.mit.edu/vision/datasets/ADE20K/terms.

[37] Mahyar Najibi, Bharat Singh, and Larry S Davis. Autofocus: Efficient multi-scale inference. In *Proceedings of the IEEE/CVF international conference on computer vision*, pages 9745–9755, 2019.

[38] Yongming Rao, Wenliang Zhao, Benlin Liu, Jiwen Lu, Jie Zhou, and Cho-Jui Hsieh. Dynamicvit: Efficient vision transformers with dynamic token sparsification. *Advances in neural information processing systems*, 34:13937–13949, 2021.

[39] Bharat Singh and Larry S Davis. An analysis of scale invariance in object detection snip. In *Proceedings of the IEEE conference on computer vision and pattern recognition*, pages 3578–3587, 2018.

[40] Bharat Singh, Mahyar Najibi, and Larry S Davis. Sniper: Efficient multi-scale training. *Advances in neural information processing systems*, 31, 2018.

[41] Andreas Steiner, Alexander Kolesnikov, Xiaohua Zhai, Ross Wightman, Jakob Uszkoreit, and Lucas Beyer. How to train your vit? data, augmentation, and regularization in vision transformers. *arXiv preprint arXiv:2106.10270*, 2021.

[42] Mingxing Tan, Ruoming Pang, and Quoc V Le. Efficientdet: Scalable and efficient object detection. In *Proceedings of the IEEE/CVF conference on computer vision and pattern recognition*, pages 10781–10790, 2020.

[43] Hugo Touvron, Matthieu Cord, Matthijs Douze, Francisco Massa, Alexandre Sablayrolles, and Herve Jegou. Training data-efficient image transformers & distillation through attention. In *International Conference on Machine Learning*, volume 139, pages 10347–10357, July 2021.

[44] Hugo Touvron, Matthieu Cord, and Hervé Jégou. Deit iii: Revenge of the vit. In *European conference on computer vision*, pages 516–533. Springer, 2022.

[45] Princeton University and Stanford University. Imagenet terms & conditions of use. `https://image-net.org/download`.

[46] Jingdong Wang, Ke Sun, Tianheng Cheng, Borui Jiang, Chaorui Deng, Yang Zhao, Dong Liu, Yadong Mu, Mingkui Tan, Xinggang Wang, et al. Deep high-resolution representation learning for visual recognition. *IEEE transactions on pattern analysis and machine intelligence*, 43(10):3349–3364, 2020.

[47] Sinong Wang, Belinda Z Li, Madian Khabsa, Han Fang, and Hao Ma. Linformer: Self-attention with linear complexity. *arXiv preprint arXiv:2006.04768*, 2020.

[48] Wenhai Wang, Jifeng Dai, Zhe Chen, Zhenhang Huang, Zhiqi Li, Xizhou Zhu, Xiaowei Hu, Tong Lu, Lewei Lu, Hongsheng Li, et al. Internimage: Exploring large-scale vision foundation models with deformable convolutions. In *Proceedings of the IEEE/CVF Conference on Computer Vision and Pattern Recognition*, pages 14408–14419, 2023.

[49] Wenhai Wang, Enze Xie, Xiang Li, Deng-Ping Fan, Kaitao Song, Ding Liang, Tong Lu, Ping Luo, and Ling Shao. Pyramid vision transformer: A versatile backbone for dense prediction without convolutions. In *Proceedings of the IEEE/CVF international conference on computer vision*, pages 568–578, 2021.

[50] Qinrou Wen, Jirui Yang, Xue Yang, and Kewei Liang. Patchdct: Patch refinement for high quality instance segmentation. In *The Eleventh International Conference on Learning Representations*, 2022.

[51] Yuxin Wu and Kaiming He. Group normalization. In *Proceedings of the European conference on computer vision*, pages 3–19, 2018.

[52] Chunlong Xia, Xinliang Wang, Feng Lv, Xin Hao, and Yifeng Shi. Vit-comer: Vision transformer with convolutional multi-scale feature interaction for dense predictions. In *Proceedings of the IEEE/CVF conference on computer vision and pattern recognition*, 2024.

[53] Zhuofan Xia, Xuran Pan, Shiji Song, Li Erran Li, and Gao Huang. Vision transformer with deformable attention. In *Proceedings of the IEEE/CVF conference on computer vision and pattern recognition*, pages 4794–4803, 2022.

[54] Tete Xiao, Yingcheng Liu, Bolei Zhou, Yuning Jiang, and Jian Sun. Unified perceptual parsing for scene understanding. In *Proceedings of the European conference on computer vision*, pages 418–434, 2018.

[55] Yifan Xu, Zhijie Zhang, Mengdan Zhang, Kekai Sheng, Ke Li, Weiming Dong, Liqing Zhang, Changsheng Xu, and Xing Sun. Evo-vit: Slow-fast token evolution for dynamic vision transformer. In *Proceedings of the AAAI Conference on Artificial Intelligence*, volume 36, pages 2964–2972, 2022.

[56] Xue Yang, Junchi Yan, Ziming Feng, and Tao He. R3det: Refined single-stage detector with feature refinement for rotating object. In *Proceedings of the AAAI conference on artificial intelligence*, volume 35, pages 3163–3171, 2021.

[57] Xue Yang, Jirui Yang, Junchi Yan, Yue Zhang, Tengfei Zhang, Zhi Guo, Xian Sun, and Kun Fu. Scrdet: Towards more robust detection for small, cluttered and rotated objects. In *Proceedings of the IEEE/CVF international conference on computer vision*, pages 8232–8241, 2019.

[58] Yuhui Yuan, Rao Fu, Lang Huang, Weihong Lin, Chao Zhang, Xilin Chen, and Jingdong Wang. Hrformer: High-resolution vision transformer for dense prediction. *Advances in Neural Information Processing Systems*, 34, 2021.

[59] Hao Zhang, Feng Li, Shilong Liu, Lei Zhang, Hang Su, Jun Zhu, Lionel M Ni, and Heung-Yeung Shum. Dino: Detr with improved denoising anchor boxes for end-to-end object detection. In *International Conference on Learning Representations*, 2022.

[60] Kaipeng Zhang, Zhanpeng Zhang, Zhifeng Li, and Yu Qiao. Joint face detection and alignment using multitask cascaded convolutional networks. *IEEE signal processing letters*, 23(10):1499–1503, 2016.

[61] Tianwen Zhang, Xiaoling Zhang, and Xiao Ke. Quad-fpn: A novel quad feature pyramid network for sar ship detection. *Remote Sensing*, 13(14):2771, 2021.

[62] Bolei Zhou, Hang Zhao, Xavier Puig, Sanja Fidler, Adela Barriuso, and Antonio Torralba. Scene parsing through ade20k dataset. In *Proceedings of the IEEE/CVF conference on computer vision and pattern recognition*, pages 633–641, 2017.

[63] Xizhou Zhu, Weijie Su, Lewei Lu, Bin Li, Xiaogang Wang, and Jifeng Dai. Deformable detr: Deformable transformers for end-to-end object detection. In *International Conference on Learning Representations*, 2020.

[64] Zhuofan Zong, Guanglu Song, and Yu Liu. Detrs with collaborative hybrid assignments training. In *Proceedings of the IEEE/CVF international conference on computer vision*, pages 6748–6758, 2023.

A Appendix

A.1 Detailed Training Settings for Image Classification

Detailed training settings for image classification are provided in Table 11.

A.2 Full Detection Results

Full results of Fig. 4 are provided in Table 12.

Table 11: Detailed training setting for image classification.

batch size	1024
epochs	20
optimizer	AdamW
weight decay	0.1
learning rate scheduler	cosine
initial learning rate	3e-5
warmup epochs	5
mixup	0.8
cutmix	1.0
random erasing	0
auto augment	✓
color jitter	0.3
label smoothing	0.1
dropout	✗
drop path rate	0.4 (ViT-L) / 0.2 (ViT-B) / 0.05 (ViT-S, ViT-T)
repeated aug	✗
gradient clip	✗
loss	cross entropy

A.3 Broader Impacts

Our method helps to save computational overheads of large-scale vision foundation models such as InternViT-6B, therefore reducing energy consumption. This may bring positive impacts on carbon emissions reduction and contribute to environmental sustainability. However, energy consumption of large models still needs to be treated with caution.

Table 12: Full results of PIIP variants under different resolution configurations.

Model	Resolution	#FLOPs	Mask R-CNN 1× schedule							
			AP^b	AP^b_l	AP^b_m	AP^b_s	AP^m	AP^m_l	AP^m_m	AP^m_s
PIIP-TSB	896/672/448	176G	42.1	62.2	46.8	20.8	36.9	60.9	40.2	13.7
	1120/672/448	192G	42.7	62.3	46.9	22.7	37.9	61.2	40.9	15.4
	1344/672/448	212G	43.5	62.1	47.2	23.5	38.9	60.9	41.7	16.2
	1120/896/448	243G	43.9	62.4	47.9	24.4	38.6	60.8	41.9	16.6
	1344/896/448	263G	44.5	62.1	48.3	24.9	39.5	61.1	42.6	17.5
	1568/896/448	287G	45.0	62.0	48.4	26.2	40.2	61.4	43.3	19.0
	1568/896/672	387G	45.8	62.9	49.9	27.2	40.7	62.3	44.1	19.5
	1568/1120/672	453G	46.6	63.1	50.9	28.5	41.4	62.3	45.0	20.6
	1792/1120/672	480G	46.7	63.0	50.6	29.0	41.7	62.5	45.0	20.5
	1792/1344/672	561G	46.8	62.5	50.8	30.1	42.0	62.5	45.1	21.8
PIIP-SBL	672/448/224	245G	41.1	63.6	45.8	18.4	35.3	61.5	38.4	10.7
	896/448/224	298G	43.5	63.9	47.8	21.9	37.7	62.4	41.1	14.3
	1120/448/224	367G	45.2	63.7	49.4	25.2	39.6	62.9	42.9	16.7
	1120/672/224	504G	45.8	64.7	50.0	26.1	40.3	63.3	43.8	17.4
	1120/672/448	727G	46.7	63.0	50.6	29.0	40.8	64.4	44.1	18.1
	1344/672/448	811G	47.5	65.8	51.7	27.6	42.0	64.7	45.7	19.5
	1344/896/448	1002G	48.2	66.2	52.5	28.8	42.5	65.3	46.2	20.1
	1568/896/672	1464G	49.4	66.5	53.9	30.6	43.7	64.9	47.5	22.0
	1568/1120/672	1709G	49.9	66.9	54.3	31.7	44.3	65.3	48.0	22.9
	1792/1120/672	1824G	49.9	65.9	54.3	32.0	44.6	65.4	48.3	23.1
PIIP-TSBL	1344/896/672/448	755G	46.9	65.5	50.4	27.8	41.6	64.4	44.7	19.5
	1568/1120/672/448	861G	48.2	66.1	52.0	29.4	42.8	64.7	46.0	21.0
	1568/1120/896/448	1052G	48.7	66.4	52.4	30.2	43.4	65.2	46.7	21.4
	1792/1344/896/448	1180G	49.0	65.9	52.7	30.5	43.7	65.0	47.0	22.4
	1792/1568/1120/448	1535G	49.6	65.7	53.1	32.1	44.2	65.2	47.5	22.9

A.4 Licenses of Datasets

ImageNet-1k [11] is subject to the ImageNet terms of use [45].

COCO [28] is subject to the Flickr terms of use [15].

ADE20K [62] is subject to the ADE20K terms of use [36].

NeurIPS Paper Checklist

1. **Claims**

   Question: Do the main claims made in the abstract and introduction accurately reflect the paper's contributions and scope?

   Answer: [Yes]

   Justification: The contributions are stated in the abstract and introduction.

   Guidelines:

   - The answer NA means that the abstract and introduction do not include the claims made in the paper.
   - The abstract and/or introduction should clearly state the claims made, including the contributions made in the paper and important assumptions and limitations. A No or NA answer to this question will not be perceived well by the reviewers.
   - The claims made should match theoretical and experimental results, and reflect how much the results can be expected to generalize to other settings.
   - It is fine to include aspirational goals as motivation as long as it is clear that these goals are not attained by the paper.

2. **Limitations**

   Question: Does the paper discuss the limitations of the work performed by the authors?

   Answer: [Yes]

   Justification: The limitations are discussed in the conclusion section.

   Guidelines:

   - The answer NA means that the paper has no limitation while the answer No means that the paper has limitations, but those are not discussed in the paper.
   - The authors are encouraged to create a separate "Limitations" section in their paper.
   - The paper should point out any strong assumptions and how robust the results are to violations of these assumptions (e.g., independence assumptions, noiseless settings, model well-specification, asymptotic approximations only holding locally). The authors should reflect on how these assumptions might be violated in practice and what the implications would be.
   - The authors should reflect on the scope of the claims made, e.g., if the approach was only tested on a few datasets or with a few runs. In general, empirical results often depend on implicit assumptions, which should be articulated.
   - The authors should reflect on the factors that influence the performance of the approach. For example, a facial recognition algorithm may perform poorly when image resolution is low or images are taken in low lighting. Or a speech-to-text system might not be used reliably to provide closed captions for online lectures because it fails to handle technical jargon.
   - The authors should discuss the computational efficiency of the proposed algorithms and how they scale with dataset size.
   - If applicable, the authors should discuss possible limitations of their approach to address problems of privacy and fairness.
   - While the authors might fear that complete honesty about limitations might be used by reviewers as grounds for rejection, a worse outcome might be that reviewers discover limitations that aren't acknowledged in the paper. The authors should use their best judgment and recognize that individual actions in favor of transparency play an important role in developing norms that preserve the integrity of the community. Reviewers will be specifically instructed to not penalize honesty concerning limitations.

3. **Theory Assumptions and Proofs**

   Question: For each theoretical result, does the paper provide the full set of assumptions and a complete (and correct) proof?

   Answer: [NA]

Justification: This paper does not include theoretical results.

Guidelines:

- The answer NA means that the paper does not include theoretical results.
- All the theorems, formulas, and proofs in the paper should be numbered and cross-referenced.
- All assumptions should be clearly stated or referenced in the statement of any theorems.
- The proofs can either appear in the main paper or the supplemental material, but if they appear in the supplemental material, the authors are encouraged to provide a short proof sketch to provide intuition.
- Inversely, any informal proof provided in the core of the paper should be complemented by formal proofs provided in appendix or supplemental material.
- Theorems and Lemmas that the proof relies upon should be properly referenced.

4. **Experimental Result Reproducibility**

   Question: Does the paper fully disclose all the information needed to reproduce the main experimental results of the paper to the extent that it affects the main claims and/or conclusions of the paper (regardless of whether the code and data are provided or not)?

   Answer: [Yes]

   Justification: The details are provided in the experiment section and the appendix. Our code has been released.

   Guidelines:

   - The answer NA means that the paper does not include experiments.
   - If the paper includes experiments, a No answer to this question will not be perceived well by the reviewers: Making the paper reproducible is important, regardless of whether the code and data are provided or not.
   - If the contribution is a dataset and/or model, the authors should describe the steps taken to make their results reproducible or verifiable.
   - Depending on the contribution, reproducibility can be accomplished in various ways. For example, if the contribution is a novel architecture, describing the architecture fully might suffice, or if the contribution is a specific model and empirical evaluation, it may be necessary to either make it possible for others to replicate the model with the same dataset, or provide access to the model. In general. releasing code and data is often one good way to accomplish this, but reproducibility can also be provided via detailed instructions for how to replicate the results, access to a hosted model (e.g., in the case of a large language model), releasing of a model checkpoint, or other means that are appropriate to the research performed.
   - While NeurIPS does not require releasing code, the conference does require all submissions to provide some reasonable avenue for reproducibility, which may depend on the nature of the contribution. For example
     (a) If the contribution is primarily a new algorithm, the paper should make it clear how to reproduce that algorithm.
     (b) If the contribution is primarily a new model architecture, the paper should describe the architecture clearly and fully.
     (c) If the contribution is a new model (e.g., a large language model), then there should either be a way to access this model for reproducing the results or a way to reproduce the model (e.g., with an open-source dataset or instructions for how to construct the dataset).
     (d) We recognize that reproducibility may be tricky in some cases, in which case authors are welcome to describe the particular way they provide for reproducibility. In the case of closed-source models, it may be that access to the model is limited in some way (e.g., to registered users), but it should be possible for other researchers to have some path to reproducing or verifying the results.

5. **Open access to data and code**

Question: Does the paper provide open access to the data and code, with sufficient instructions to faithfully reproduce the main experimental results, as described in supplemental material?

Answer: [Yes]

Justification: The data is publicly available datasets. Our code has been released. Details to reproduce the experiments is described in the experiments section and the appendix.

Guidelines:

- The answer NA means that paper does not include experiments requiring code.
- Please see the NeurIPS code and data submission guidelines (`https://nips.cc/public/guides/CodeSubmissionPolicy`) for more details.
- While we encourage the release of code and data, we understand that this might not be possible, so No is an acceptable answer. Papers cannot be rejected simply for not including code, unless this is central to the contribution (e.g., for a new open-source benchmark).
- The instructions should contain the exact command and environment needed to run to reproduce the results. See the NeurIPS code and data submission guidelines (`https://nips.cc/public/guides/CodeSubmissionPolicy`) for more details.
- The authors should provide instructions on data access and preparation, including how to access the raw data, preprocessed data, intermediate data, and generated data, etc.
- The authors should provide scripts to reproduce all experimental results for the new proposed method and baselines. If only a subset of experiments are reproducible, they should state which ones are omitted from the script and why.
- At submission time, to preserve anonymity, the authors should release anonymized versions (if applicable).
- Providing as much information as possible in supplemental material (appended to the paper) is recommended, but including URLs to data and code is permitted.

6. **Experimental Setting/Details**

   Question: Does the paper specify all the training and test details (e.g., data splits, hyperparameters, how they were chosen, type of optimizer, etc.) necessary to understand the results?

   Answer: [Yes]

   Justification: Training details are in the experiment section and appendix.

   Guidelines:

   - The answer NA means that the paper does not include experiments.
   - The experimental setting should be presented in the core of the paper to a level of detail that is necessary to appreciate the results and make sense of them.
   - The full details can be provided either with the code, in appendix, or as supplemental material.

7. **Experiment Statistical Significance**

   Question: Does the paper report error bars suitably and correctly defined or other appropriate information about the statistical significance of the experiments?

   Answer: [No]

   Justification: Calculating error bars would be too computational expensive, given the size of the model and the dataset.

   Guidelines:

   - The answer NA means that the paper does not include experiments.
   - The authors should answer "Yes" if the results are accompanied by error bars, confidence intervals, or statistical significance tests, at least for the experiments that support the main claims of the paper.
   - The factors of variability that the error bars are capturing should be clearly stated (for example, train/test split, initialization, random drawing of some parameter, or overall run with given experimental conditions).

- The method for calculating the error bars should be explained (closed form formula, call to a library function, bootstrap, etc.)
- The assumptions made should be given (e.g., Normally distributed errors).
- It should be clear whether the error bar is the standard deviation or the standard error of the mean.
- It is OK to report 1-sigma error bars, but one should state it. The authors should preferably report a 2-sigma error bar than state that they have a 96% CI, if the hypothesis of Normality of errors is not verified.
- For asymmetric distributions, the authors should be careful not to show in tables or figures symmetric error bars that would yield results that are out of range (e.g. negative error rates).
- If error bars are reported in tables or plots, The authors should explain in the text how they were calculated and reference the corresponding figures or tables in the text.

8. **Experiments Compute Resources**

   Question: For each experiment, does the paper provide sufficient information on the computer resources (type of compute workers, memory, time of execution) needed to reproduce the experiments?

   Answer: [Yes]

   Justification: Details are in the experiment section and the appendix.

   Guidelines:

   - The answer NA means that the paper does not include experiments.
   - The paper should indicate the type of compute workers CPU or GPU, internal cluster, or cloud provider, including relevant memory and storage.
   - The paper should provide the amount of compute required for each of the individual experimental runs as well as estimate the total compute.
   - The paper should disclose whether the full research project required more compute than the experiments reported in the paper (e.g., preliminary or failed experiments that didn't make it into the paper).

9. **Code Of Ethics**

   Question: Does the research conducted in the paper conform, in every respect, with the NeurIPS Code of Ethics https://neurips.cc/public/EthicsGuidelines?

   Answer: [Yes]

   Justification: the paper conforms the code of ethics.

   Guidelines:

   - The answer NA means that the authors have not reviewed the NeurIPS Code of Ethics.
   - If the authors answer No, they should explain the special circumstances that require a deviation from the Code of Ethics.
   - The authors should make sure to preserve anonymity (e.g., if there is a special consideration due to laws or regulations in their jurisdiction).

10. **Broader Impacts**

    Question: Does the paper discuss both potential positive societal impacts and negative societal impacts of the work performed?

    Answer: [Yes]

    Justification: Broader impacts are discussed in the appendix.

    Guidelines:

    - The answer NA means that there is no societal impact of the work performed.
    - If the authors answer NA or No, they should explain why their work has no societal impact or why the paper does not address societal impact.
    - Examples of negative societal impacts include potential malicious or unintended uses (e.g., disinformation, generating fake profiles, surveillance), fairness considerations (e.g., deployment of technologies that could make decisions that unfairly impact specific groups), privacy considerations, and security considerations.

- The conference expects that many papers will be foundational research and not tied to particular applications, let alone deployments. However, if there is a direct path to any negative applications, the authors should point it out. For example, it is legitimate to point out that an improvement in the quality of generative models could be used to generate deepfakes for disinformation. On the other hand, it is not needed to point out that a generic algorithm for optimizing neural networks could enable people to train models that generate Deepfakes faster.
- The authors should consider possible harms that could arise when the technology is being used as intended and functioning correctly, harms that could arise when the technology is being used as intended but gives incorrect results, and harms following from (intentional or unintentional) misuse of the technology.
- If there are negative societal impacts, the authors could also discuss possible mitigation strategies (e.g., gated release of models, providing defenses in addition to attacks, mechanisms for monitoring misuse, mechanisms to monitor how a system learns from feedback over time, improving the efficiency and accessibility of ML).

11. **Safeguards**

    Question: Does the paper describe safeguards that have been put in place for responsible release of data or models that have a high risk for misuse (e.g., pretrained language models, image generators, or scraped datasets)?

    Answer: [NA]

    Justification: The paper poses no such risks.

    Guidelines:

    - The answer NA means that the paper poses no such risks.
    - Released models that have a high risk for misuse or dual-use should be released with necessary safeguards to allow for controlled use of the model, for example by requiring that users adhere to usage guidelines or restrictions to access the model or implementing safety filters.
    - Datasets that have been scraped from the Internet could pose safety risks. The authors should describe how they avoided releasing unsafe images.
    - We recognize that providing effective safeguards is challenging, and many papers do not require this, but we encourage authors to take this into account and make a best faith effort.

12. **Licenses for existing assets**

    Question: Are the creators or original owners of assets (e.g., code, data, models), used in the paper, properly credited and are the license and terms of use explicitly mentioned and properly respected?

    Answer: [Yes]

    Justification: Datasets are referenced. License are provided in the appendix.

    Guidelines:

    - The answer NA means that the paper does not use existing assets.
    - The authors should cite the original paper that produced the code package or dataset.
    - The authors should state which version of the asset is used and, if possible, include a URL.
    - The name of the license (e.g., CC-BY 4.0) should be included for each asset.
    - For scraped data from a particular source (e.g., website), the copyright and terms of service of that source should be provided.
    - If assets are released, the license, copyright information, and terms of use in the package should be provided. For popular datasets, `paperswithcode.com/datasets` has curated licenses for some datasets. Their licensing guide can help determine the license of a dataset.
    - For existing datasets that are re-packaged, both the original license and the license of the derived asset (if it has changed) should be provided.

- If this information is not available online, the authors are encouraged to reach out to the asset's creators.

13. **New Assets**

    Question: Are new assets introduced in the paper well documented and is the documentation provided alongside the assets?

    Answer: [Yes]

    Justification: Documentation is be provided along with the code and models.

    Guidelines:

    - The answer NA means that the paper does not release new assets.
    - Researchers should communicate the details of the dataset/code/model as part of their submissions via structured templates. This includes details about training, license, limitations, etc.
    - The paper should discuss whether and how consent was obtained from people whose asset is used.
    - At submission time, remember to anonymize your assets (if applicable). You can either create an anonymized URL or include an anonymized zip file.

14. **Crowdsourcing and Research with Human Subjects**

    Question: For crowdsourcing experiments and research with human subjects, does the paper include the full text of instructions given to participants and screenshots, if applicable, as well as details about compensation (if any)?

    Answer: [NA]

    Justification: The paper does not involve crowdsourcing nor research with human subjects.

    Guidelines:

    - The answer NA means that the paper does not involve crowdsourcing nor research with human subjects.
    - Including this information in the supplemental material is fine, but if the main contribution of the paper involves human subjects, then as much detail as possible should be included in the main paper.
    - According to the NeurIPS Code of Ethics, workers involved in data collection, curation, or other labor should be paid at least the minimum wage in the country of the data collector.

15. **Institutional Review Board (IRB) Approvals or Equivalent for Research with Human Subjects**

    Question: Does the paper describe potential risks incurred by study participants, whether such risks were disclosed to the subjects, and whether Institutional Review Board (IRB) approvals (or an equivalent approval/review based on the requirements of your country or institution) were obtained?

    Answer: [NA]

    Justification: The paper does not involve crowdsourcing nor research with human subjects.

    Guidelines:

    - The answer NA means that the paper does not involve crowdsourcing nor research with human subjects.
    - Depending on the country in which research is conducted, IRB approval (or equivalent) may be required for any human subjects research. If you obtained IRB approval, you should clearly state this in the paper.
    - We recognize that the procedures for this may vary significantly between institutions and locations, and we expect authors to adhere to the NeurIPS Code of Ethics and the guidelines for their institution.
    - For initial submissions, do not include any information that would break anonymity (if applicable), such as the institution conducting the review.